Chalcogenide Letters Vol. 9, No. 4, April 2012, p. 157 - 163

IMPACT OF THE MORPHOLOGY OF TiO_2 FILMS AS CATHODE BUFFER LAYER ON THE EFFICIENCY OF INVERTED-STRUCTURE POLYMER SOLAR CELLS

ORAWAN WIRANWETCHAYAN[a,b], QIFENG ZHANG[a], XIAOYUAN ZHOU[a], ZHIQIANG LIANG[a], PISITH SINGJAI[b], GUOZHONG CAO[a*]

[a]*Department of Materials Science and Engineering, University of Washington, Seattle, WA 98195, USA*

[b]*Department of Physics and Material Science, Faculty of Science, Chiang Mai University, Chiang Mai 50200, Thailand*

Semiconducting metal-oxide TiO_2 films were deposited on FTO substrates via a sol-gel method to fabricate inverted polymer solar cells. The pore size of the TiO_2 films was effectively controlled by using the sols different in stirring time. The solar cell was constructed with a fullerene derivative interlayer and a photoactive mixture of poly(3-hexylthiophene) (P3HT) and phenyl-C61-butyric acid methyl ester (PCBM) coated on the TiO_2 films, which were purposely fabricated to have different porosity, referred as dense film, mesoporous film, and macroporous film in this paper. The highest efficiency, ~3.4%, was achieved on the cell with mesoporous film as the cathode buffer layer. It was proposed that, compared with the case of dense film, the mesoporous film leading to power conversion efficiency enhancement resulted from the efficient charge separation introduced by increasing the interface area between an active layer and metal oxide films and thus lowering the recombination rate happened to the excited electrons with holes in the polymer. The cell with macroporous film showing a much low efficiency is attributed to electron trapping during the transport in large grains, leading to lowly efficient electron collection.

(Received March 2, 2012; Accepted April 24, 2012)

1. Introduction

Polymer solar cells (or organic photovoltaic) are devices that are based on conjugated polymers and can convert radiation from the sun to electricity,[1-4] and have attracted great interest as a cleaner source of energy.[5-8] An efficiency of 7.4% has been reported for bulk heterojunction polymer solar cells with conventional device structures.[9] However, conventional solar cells can suffer from both cathode degradation in view of their sensitivity to the oxygen and moisture in air and anode degradation due to the etching of PEDOT to ITO film. Therefore, these devices exhibit short lifetimes. [10-12] To achieve higher device efficiencies and increased stability, high hole mobility, high photosensitivity in the polymer, and high carrier mobility and good stability in the inorganic semiconductors are properties that must be maximized in the development of solar cells. Polymer solar cells with inverted device structure are an alternative solution to improve the longevity, because they use a more air-stable, high work-function electrode such as Ag or Au as a back contact to collect holes, while using an inorganic semiconductor as the buffer layer to collect electrons and meanwhile avoid the contact of ITO film with PEDOT polymer.[13-18]

Inverted structure polymer solar cells often consist of nanocrystalline inorganic semiconductor oxides such as ZnO or TiO_2 as cathode buffer layer, with various morphologies—such as mesoporous structures, [16-22] nanotube arrays, [23-26] or nanorod structures [14,27-30]—in contact with the conjugated polymer. One of the most commonly used combinations is poly(3-

*Correspondence: gzcao@u.washington.edu

hexylthiophene) (P3HT) with [6,6]-phenyl-C61-butyric acid methyl (PCBM). In polymer solar cells, interaction between the incident photons and the conjugated polymer generates excitons. The excitons move to and become disassociated at the interface of P3HT and PCBM, which function as electron-donor and electron-acceptor, respectively. Electrons are then carried through the acceptor material, pass through the cathode buffer layer, and reach the collecting electrode (i.e., typically ITO film), as holes are transferred through the donor material, pass through a hole transport layer (e.g., PEDOT), and eventually reach the metal electrode. In an inverted structure polymer solar cell, the cathode buffer layer is adopted to prevent the recombination between the holes in the donor material and the electrons in the collecting electrode. This is achieved by either enabling the formation of a continuous film of PCBM [31] or, as suggested in some literature, establishing an energy barrier between the polymers and the ITO film.[32] Moreover, it has been found that the morphology of the cathode buffer layer may have a significant impact on the solar cell efficiency.

In this work, TiO_2 films different in morphology as well as roughness were fabricated on fluorine-doped tin oxide (FTO) substrates via a sol-gel method to work as cathode buffer layer in inverted structure polymer solar cells. The roughness of the TiO_2 films was carefully controlled by adjusting the aging time of TiO_2 sol for the film fabrication. It would be shown that the solar cells based on P3HT and PCBM with porous TiO_2 film as cathode buffer layer present higher efficiency than dense films as the cathode buffer layer. The highest efficiency was achieved on the cell using mesoporous TiO_2 film with pore size of ~20 nm.

2. Experimental details

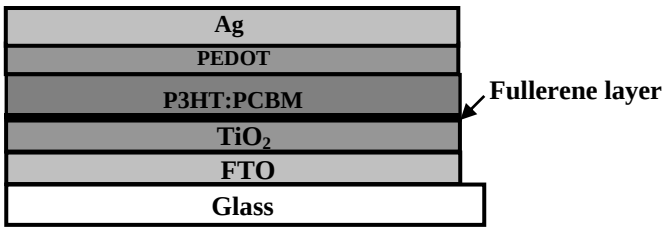

Fig. 1 Schematic showing the configuration of an inverted hybrid solar cell

Synthesis of metal oxide films.

Preparation of TiO_2 sol for dense film: Titanium isopropoxide [$Ti(OC_3H_7)_4$, TTIP] was used for the preparation of TiO_2 sol. Typically, 0.1 mL of acetic acid and 15 mL of ethanol were dropwise added to 0.7 mL of TTIP. The solutions were mixed in a glass container by stirring for 30 min without heating, resulting in formation of a TiO_2 sol in light yellow color. The solution was kept for aging for at least three days prior to use.

Preparation of TiO_2 sol for porous films: The solution was prepared by mixing 1.5 mL of acetic acid and 2 mL of ethanol with 0.75 mL of TTIP. The as-prepared sol was used for the fabrication of mesoporous TiO_2 film in this paper. For the sol to make macroporous film, 0.3 g of PVP and 3.5 mL of ethanol were added to the aforementioned TiO_2 sol. The resulting light yellow solution with 30-60 minutes of stirring was transparent without precipitation. However, it was found that the solution suffering different stirring time might have a significant impact on the porosity of the TiO_2 film produced with a spin coating method.

The FTO substrates were cleaned by sonication with acetone, DI water and isopropanol. The sols of TiO_2 were employed to form films onto the FTO substrate through a spin coating method. The as-prepared TiO_2 films then suffered a heat treatment at 450 ^oC for 1 h in order to eliminate the organic components and to activate the crystallization of the TiO_2. The surface morphology was studied using a scanning electron microscope (SEM, Philips, JEOL JSM7000). Crystallographic characterizations of the samples were performed with a Bruker D8 Focus X-ray diffractometer.

Device fabrication and characterization. First, the substrates with TiO_2 film were pre-treated with oxygen plasma for 10 min. The fullerene [18] of a dichlorometane solution containing 20 mg/mL of PCBM (American Dye Source Inc. ADS61BFB) was spin coated onto the mp-TiO_2 at a rate of 1000 rpm for 30 s in a glovebox, and then annealed at 250 °C for 1 min to help the infiltration of the polymer into the mp-TiO_2 films. Subsequently, the chlorodebenzene solution containing 20 mg mL^{-1} P3HT (Reike Metal, Sepiolid P100) and 20 mg mL^{-1} PCBM, which was stirred inside a glovebox overnight at 60˚C and then filtered with a 0.2 μm polytetrafluoroethylene (PTFE) filter, was spin coated onto the FTO glass substrates coated with TiO_2 films and fullerene interlayer at 1,000 rpm for 30 s. The samples were then baked at 225 °C for 1 min to remove residual solvent and improve the contact between the polymer and oxide film to some extent. A poly(3,4-ethylene-dioxylene thiophene):poly(styrene sulfonic acid) (PEDOT:PSS, Clevios P VP Al 4083) was mixed with absolute isopropanol and butanol at a volume ratio of 1 : 2 : 2.[14] The solution was subsequently spin-coated onto the P3HT/PCBM film to form a hole-transport layer. The substrates were then heated at 120˚C for 10 min. Finally, a 100 nm thick silver film was deposited on the PEDOT:PSS under vacuum to work as top electrode. The structure of the device is illustrated in Fig.1. The *J-V* characteristics of the solar cells were measured in the glovebox using a Keithley 2400 source measurement unit, and an Oriel Xenon lamp (450W) coupled with an AM1.5 filter. A calibrated silicon reference solar cell certified by the National Renewable Energy Laboratory (NREL) was used to confirm the measurement conditions. A light intensity of 100 mW cm^{-2} was used in all the measurements in this study.

3. Results and discussion

Fig. 2 shows top-view scanning electron microscopy (SEM) images of (a) dense TiO_2, (b) mesoporous TiO_2, and (c) macroporous TiO_2 films, respectively. The image of Figure 2a shows that a densely packed TiO_2 film is successfully fabricated on the FTO glass substrate. The image of Figures 2b and c show the SEM images of TiO_2 films with different porosity by adopting different stirring time to the mixture solution of TiO_2 and PVP. It can be seen that the pore diameter was about 20-50 nm for the film produced with the solution with 60 minutes of stirring, and 10-20 nm for 30 minutes of stirring. Figure 2c shows the cross section SEM of an inverted structure solar cell using a porous TiO_2 films.

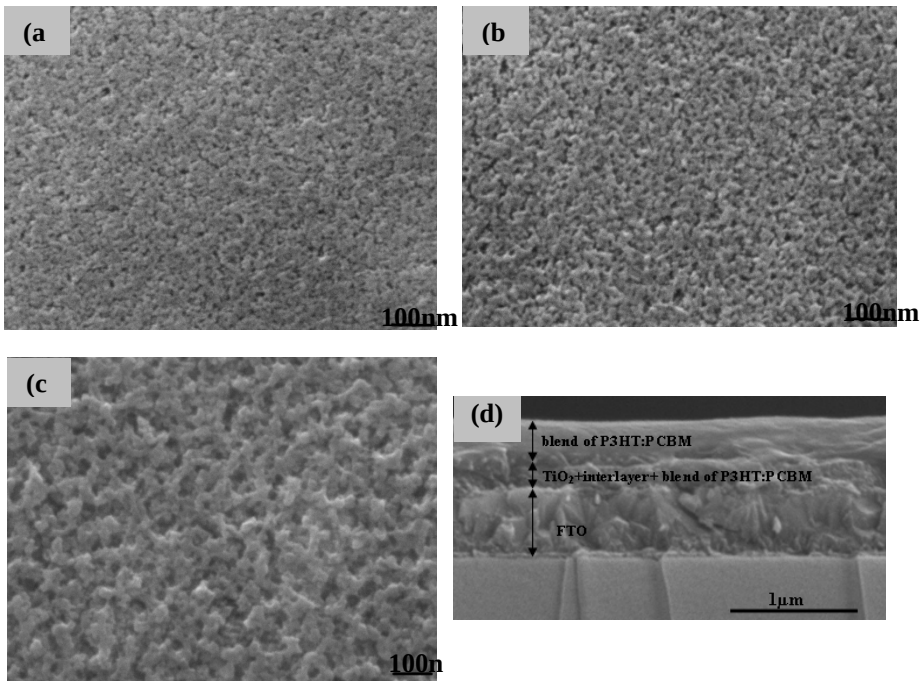

Fig. 2. Top-view scanning electron microscopy (SEM) images of (a) dense TiO_2, (b) mesoporousTiO_2, and (c) macroporousTiO_2 films, respectively. The scale bar represents 100 nm. (d) The cross section SEM of an inverted structure solar cell using a porous TiO_2 films.

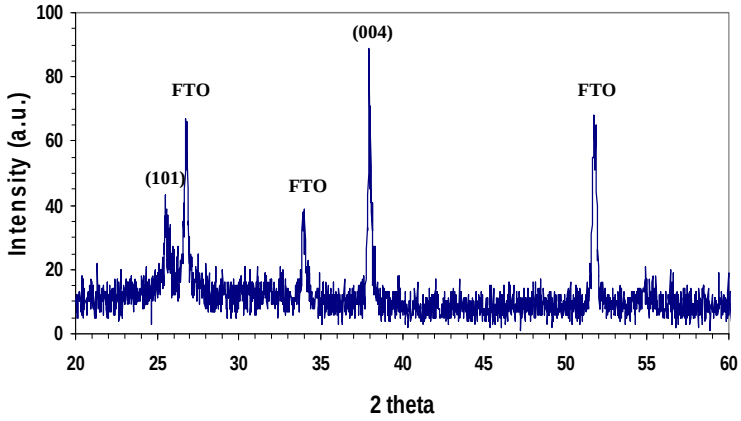

Fig. 3. XRD patterns for the TiO_2 films

Fig. 3 shows XRD pattern for the TiO_2 dense film after annealed at 450 ˚C for 1h in air, indicating an anatase phase of TiO_2 produced with the as-prepared sol (JCPDS Card no. 84-1286).

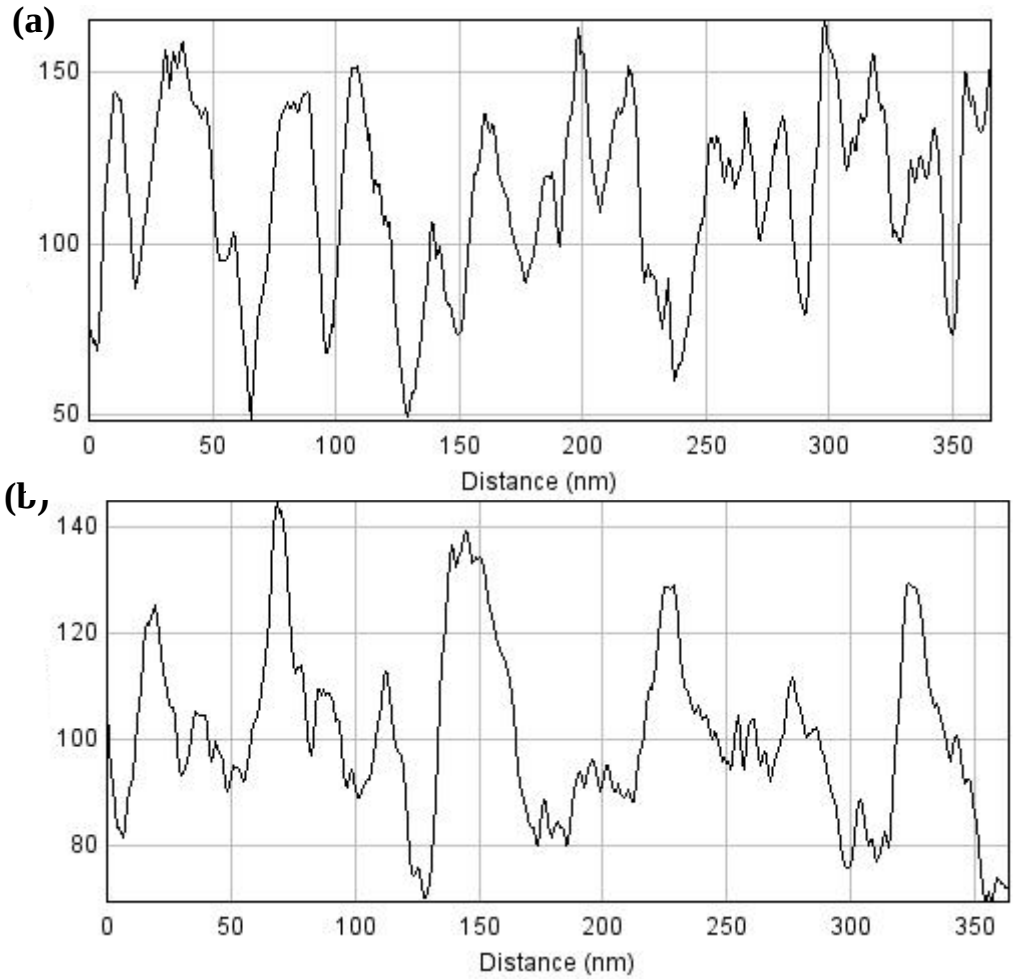

Fig. 4. Line scan profile of (a) mesoporous TiO_2 films and (b) macroporous TiO_2.Analysis performed using ImageJ.

Fig. 4 shows the line scan profiles for the mesoporous and macroporous TiO_2 films. The roughness of the macroporous TiO_2 was shown to be larger than that of the mesoporous TiO_2.

The characteristic current density(J)-voltage(V) plots shown in Figure 5 gave the short-circuit current (J_{sc}) and open-circuit voltage (V_{oc}) of the inverted structure solar cells constructured with fullerene interlayer and a blend of P3HT and PCBM using TiO_2 film as cathode buffer layer. The short-circuit current density (J_{sc}), open-circuit voltage (V_{oc}), fill factor (FF), and overall power conversion efficiency (η) values are summarized in Table I. The maximum efficiency was obtained with mesoporous TiO_2 films with a pore size of ~10-20 nm. The highest hybrid solar cell performance was achieved with values of V_{oc}= 0.602 V, J_{sc}=9.03 mA/cm^2, FF=62.0%, η=3.4%. The solar cells based on dense TiO_2 and macroporous TiO_2 exhibited relatively low efficiencies, 1.9% and 1.7%, respectively.

Table I. Performances of solar cells with electrodes made of dense, mesoporous and macroporous TiO_2 films.

TiO_2	V_{oc}	J_{sc}	FF(%)	η(%)
	(V)	(mA-cm^{-2})		
mesoporous 10-20 nm	0.602	9.03	62.0	3.4
macroporous 20-50 nm	0.565	7.22	41.9	1.7
dense	0.595	7.02	44.9	1.9

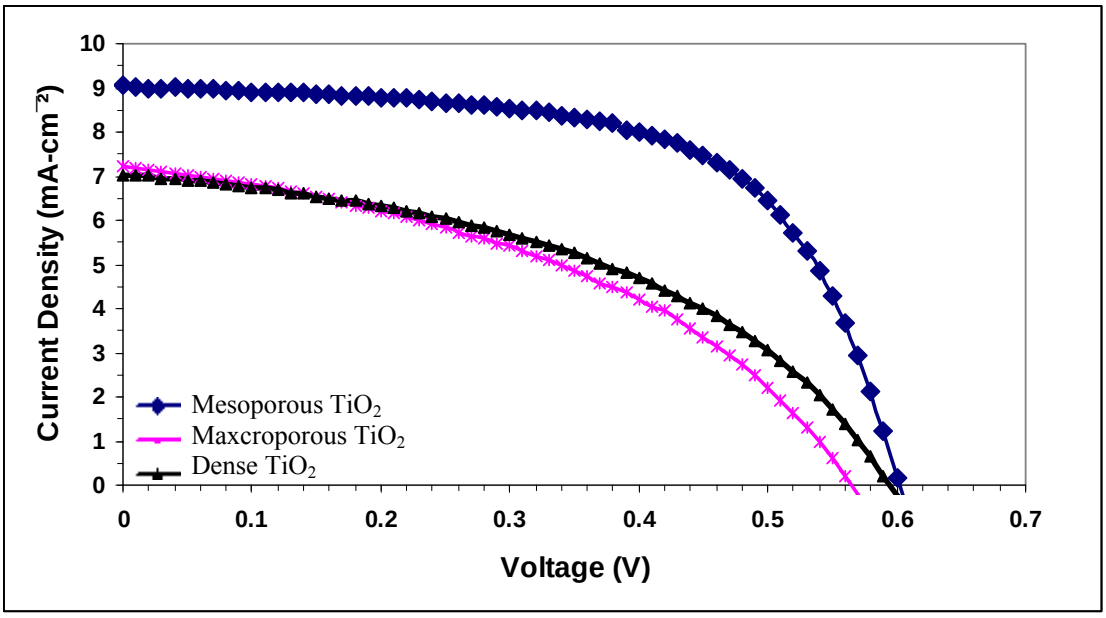

Fig. 5. Current density-voltage curves for inverted hybrid solar cells with dense, mesoporous and macroporous TiO_2 films.

It is interesting that the morphology of TiO_2 serving as cathode buffer layer may significantly affect the performance of inverted structure polymer solar cells. In our previous work, it has been revealed that the role of an oxide layer in the inverted structure polymer solar cells is to enable the formation of a continuous layer of PCBM on the conductive transparent substrate so as to prevent the recombination happening between the holes in the polymer such as P3HT and the electrons in the collecting electrode of the solar cells. We have pointed out that, in the case of a very thin oxide film (~10 nm) as cathode buffer layer, the electrons in the polymer such as PCBM

transport to the ITO or FTO collecting electrode in a way of tunneling through the oxide film instead of a diffusion within it.[31] However, while the thickness of the oxide film is in a range of 50-60 nm as the case of the present paper, the electrons will firstly have to transport into the oxide and then diffuse to the collecting electrode.[32] Such a diffusion process in the oxide film may cause a loss of electrons due to the existence of traps in the oxide. This can explain why the efficiency achieved in this paper with dense TiO_2 film (1.9%) is lower than what we reported in the previous work while the TiO_2 film was as thin as ~10 nm.[31]

Although the transport of electrons within a relatively thick oxide film may have a negative impact on the efficiency of solar cells, our result based on a comparison of different structure TiO_2 films suggests that a rational design and optimization of the structure of the cathode buffer layer, for example, by employing the nanostructured mesoporous film, can counteract the negative impact in view of the loss of electrons due to the traps and it can even enhance the electron collection efficiency compared with the case of a planar oxide film as the cathode buffer layer, leading to a high conversion efficiency of 3.4% as shown in this paper while a mesoporous film with average pore sizes of 10-20 nm is adopted. The nanostructure employed in the inverted structured polymer solar cells plays a role in stretching into the polymers and thus shortening the traveling distance of photoexcited electrons within the acceptor polymer, i.e., PCBM in this paper. In other words, the electrons may quickly transfer into the oxide film and, as a result, receive lower recombination rate in respect that the mobility of electrons in the oxide is much higher than in the polymer.[14,33] Note that the solar cell with macroporous TiO_2 film as cathode buffer layer receives the efficiency of 1.7%, lower than those for TiO_2 dense film and mesoporous film. This can be explained that the grain size the macroporous film is much larger than the diffusion length of electrons and therefore the electron transport in the macroporous film is lowly efficient due to the electron trapping. Such an experimental observation strongly suggests that the performance of inverted structure polymer solar cells is very sensitive to the structure and morphology of the cathode buffer layer, for which an optimization is significantly necessary.

4. Conclusions

Inverted structure polymer solar cells fabricated with mesoporous TiO_2 produced more photocurrent; in these devices η showed a 3.4% over the devices with dense and macroporous TiO_2 structures. This improved efficiency resulted from the efficient electron collection due to the use of nanostructured oxide as buffer layer. The excited electrons could transport to the TiO_2 before being recombined by holes.

Acknowledgements

This work is funded by the U.S. Department of Energy, Office of Basic Energy Sciences, Division of Materials Sciences, under Award No. DE-FG02-07ER46467 (Q.F.Z.). This work is also supported in part by the National Science Foundation (DMR 1035196), the Air Force Office of Scientific Research (AFOSR-MURI, FA9550-06-1-0326), the University of Washington TGIF grant, the Royalty Research Fund (RRF) from the Office of Research at University of Washington, the Washington Research Foundation, and the Intel Corporation, Office of the Higher Education Commission, Ministry of Education, Thailand. Orawan Wiranwetchayan was sup supported by CHE Ph.D. Scholarship, and partially supported by the Graduate School, Physics and Material Department, Faculty of Science, Chiang Mai University.

References

[1] P. Yang, X. Zhou, G. Z. Cao and C. K. Luscombe, J. Mater. Chem. **20**, 2612 (2010).
[2] Q. Zhang, C. S. Dandeneau; X. Zhou and G. Z. Cao, Adv. Mater. **21**, 4087 (2009).
[3] B. A. Gregg, J. Phys. Chem. B **107**, 4688 (2003).
[4]. F. C. Krebs, Sol. Energy Mater. Sol. Cells. 93, 394 (2009).

[5] Y.-H. Chang, S.-R. Tseng, C.-Y. Chen, H.-F. Meng, E.-C. Chen, S.-F. Horng and C.-S. Hsu, Organic Electronics. **10**, 741 (2009).
[6] W.-H. Baek, I. SeO, T.-S. Yoon, H. H. Lee, C. M. Yun and Y.-S. Kim, Sol. Energy Mater. Sol. Cells. **93**, 1587 (2009).
[7] C. Lungenshmied, G. Dennler, H. Neugebauer, S. N. Saricuftci, M. Glatthaar, T. Meyer A. Meyer. Sol. Energy Mater. Sol. Cells. 91, 379 (2007).
[8] C.-Y. Chou, J.-S. Huang, C.-H. Wu, C.-Y. Lee and C.-F. Lin, Sol. Energy Mater. Sol. Cells. **93**, 1608 (2009).
[9] Y. Liang, Z. Xu, J. Xia, S. T. Tsai, Y. Wu, G. Li, C. Ray and L. Yu, Adv. Mater. **22**, 1 (2010).
[10] K. Kawano, R. Pacios, D. Poplavskyy, J. Nelson, D.D.C. Bradley, J.R. Durrant, Sol. Energy Mater. Sol. **90**, 3520 (2006).
[11] F. C. Krebs, J. E. Carle´ , N. Cruys-Bagger, M. Andersen, M. R. Lilliedal, M. A. Hammond, S. Hvidt, Sol. Energ. Mater. Sol. **86**, 499 (2005).
[12] S. D. Oosterhout, M. M.Wienk, S. S. van Bavel, R. Thiedmann, L. J. A. Koster, J. Gilot, J. Loos, V. Schmidt and R. A. J. Janssen, Nature Materials **8**, 818 (2009).
[13] J. Bouclé, P. Ravirajanac, J. Nelson, J. Mater Chem. **17**, 3141-3153 (2007)
[14] S. Yodyingyong, X. Zhou, Q. Zhang, D. Triampo, B. Limketkai and G. Z. Cao, J. Phys. Chem. **114**, 21851 (2010).
[15] T. Yang, W. Cai, D. Qin, E. Wang, L. Lan, X. Gong, J. Peng, Y. Cao, J. Phys. Chem. C **114**, 6849 (2010).
[16] M. N. Shan, S. S. Wang, Z. Q. Bian b, J. P. Liu, Y. L. Zhao, Sol. Energy Mater. Sol. Cells. **93**, 1613 (2009).
[17] R. Zhu, C. Y. Jiang, B. Liu and S. Ramakrishna, Adv. Mater. **21**, 994 (2009).
[18] J. –S. Huang, C. –Y. Chou, W. –H. Lin, Sol. Energ. Mater. Sol. 94, 182 (2010).
[19] J. A. Chang, J. H. Rhee, S. H. Im, Y. H. Lee, H.-J. Kim, S. I. Seok, Md. K. Nazeeruddin, and M. Grätzel, Nano lett. **10**, 2609 (2010).
[20] E.Lancelle-Beltran, P. Prené, C. Boscher, P. Belleville, P. Buvat, and C. Sanchez, Adv. Mater. **18**, 2579 (2006).
[21] H. J. Lee, H. C. Leventis, S. A. Haque, T. Torres, M. Grätzel and Md. Khaja Nazeeruddin, J. Power Sources **196**, 596 (2011).
[22] N. J. Gerein, M. D. Fleischauer and M. J. Brett, Sol. Energy Mater. Sol. Cells **94**, 2343 (2010).
[23] G. K. Mor, S. Kim, M. Paulose, O. K. Varghese, K. Shankar, J. Basham and C. A. Grimes, Nano Lett. **9**(12), 4250 (2009).
[24] T. Rattanavoravipa, T. Sagawa and S. Yoshikawa, Sol. Energy Mater. Sol. Cells **92**, 1445 (2008).
[25] S.-I. Na, S.-S. Kim, W.-K. Hong, J.-W. Park, J. Jo, Y.-C. Nah, T. Lee and D.-Y. Kim, Electrochimica Acta **53**, 2560 (2008).
[26] K. Shankar, G. K. Mor, H. E. Prakasam, O. K. Varghese, and C. A. Grimes, Langmuir **23**, 12445 (2007).
[27] C. Y. Kuo, W. C. Tang, C. Gau, T. F. Guo and D. Z. Jeng, Appl. Phys. Lett **93**, 033307 (2008).
[28] Y.-Y. Lin, T.-H. Chu, S.-S. Li, C.-H. Chuang, C.-H. Chang, W.-F. Su, C.-P. Chang, M.-W. Chu and C.-W. Chen, J. Am. Chem. Soc. **131**, 3644 (2009).
[29] L. E. Greene, M. Law, B. D. Yuhas and P. Yang, J. Phys. Chem. C **111**, 18451 (2007).
[30] J. Bouclé, S. Chyla , M. S.P. Shaffer , J. R. Durrant , D. D.C. Bradley , J. Nelson, C. R. Physique **9**, 110 (2008).
[31] O. Wiranwetchayan , Z. Liang, Q. Zhang, G.Z. Cao, P. Singjai, Materials Sciences and Applications **2**, 1697 (2011).
[32] Z. Liang, Q. Zhang, O. Wiranwetchayan, J. Xi, Z. Yang, K. Park, C. Li, and G.Z. Cao, Adv. Func. Mater. DOI: 10.1002/adfm.
[33] Q. Zhang, S. Yodyingyong, J. Xi, D. Myers and G.Z. Cao, " Oxide nanowires for solar cell applications," Nanoscale **4**, 1436 (2012).